Radiation-induced segregation in proton-irradiated AuFe studied by Mossbauer spectroscopy

1992 J. Phys.: Condens. Matter 4 2415

(http://iopscience.iop.org/0953-8984/4/10/008)

J. Phys.: Condens. Matter 4 (1992) 2415–2428. Printed in the UK

Radiation-induced segregation in proton-irradiated AuFe studied by Mössbauer spectroscopy

Y Yoshida†‡, P Fratzl†, G Vogl†, H Höfer§ and F Dworschak§

† Institut für Festkörperphysik der Universität Wien, Strudlhofgasse 4, A-1090 Wien, Austria

§ IFF, Forschungszentrum Jülich GmbH, Postfach 1913, D-5170 Jülich, Federal Republic of Germany

Received 22 July 1991, in final form 30 October 1991

Abstract. Radiation-induced segregation is studied in dilute Au–1.0at.%Fe alloys after proton irradiation at 220 °C. After proton irradiation a new Mössbauer line appears with hyperfine parameters independent of the irradiation dose. This line is assigned to small Fe complexes, which do not correspond to substitutional Fe clusters. These complexes are segregated within or in the neighbourhood of sinks and seem to be repeated as a 'motif', together with Fe atoms on substitutional sites of the Au lattice, within the segregations. Fast interstitial Fe diffusion could be the reason for the segregation. At 5 K a large hyperfine field of 35 T is found to act at these Fe complexes. This field remains up to the temperature region of 30 K. Both this hyperfine field and the transition temperature are larger than the corresponding values for substitutional Fe atoms (21.5 and 13 K, respectively).

1. Introduction

Irradiation of alloys with fast particles not only creates defects in the material but may also affect the phase stability [1]. One such phenomenon is radiation-induced segregation. This process has been discussed by a number of authors, see e.g. [1–9]. However, scarcely anything is known about the *atomistic details* of radiation-induced segregation.

The aim of the present study is to contribute to an atomistic picture of Fe segregation in proton-irradiated AuFe using Mössbauer spectroscopy on ^{57}Fe. The particular strength of this technique is the possibility of obtaining information about *single Fe atoms* and Fe atoms in *very small complexes*, too small to be studied by scattering methods and too difficult to be identified by electron microscopy. Not only can the atomic environment of Fe as single atoms (substitutionally or interstitially) or in small clusters be deduced from the Mössbauer spectra, but the magnetism of small Fe clusters can also be studied. Moreover, it is advantageous to combine such a study with measurements of the electrical resistivity which provide integral information about Fe atoms in solution. The resistivity measurements are straightforward and a great number of data points can be taken with better resolution than by Mössbauer spectroscopy. By comparing the results of both methods—electrical resistivity and Mössbauer spectroscopy—we expect to derive a more complete picture of

‡ Present Address: Shizuoka Institute of Science and Technology, 2200-2 Toyosawa, Fukuroi 437, Japan.

0953-8984/92/102415+14$04.50

the radiation-induced segregation of Fe atoms and of the structure of the Fe atoms in the segregations.

In the present investigation, both techniques—Mössbauer spectroscopy and electrical resistivity measurements—have been applied to exactly the same samples of Au–1at.%Fe. In some of the samples, He bubbles were produced by He implantation followed by annealing at 600 °C in order to introduce additional internal sinks for the mobile defects. Indeed, AuFe appears to be an ideal system for the study of radiation-induced segregation by Mössbauer spectroscopy because:

(i) after proton irradiation at 220 °C the electrical resistivity has previously been found to decay in samples both without and with He bubbles (the decrease in the resistivity has been interpreted as a depletion of the matrix by the segregation of Fe atoms to sinks during irradiation [10]);

(ii) ^{57}Fe can be used as a Mössbauer probe and the resistivity contribution ρ_{Fe} of Fe in Au is very large;

(iii) the Mössbauer parameters, i.e. isomer shifts, and quadrupole splittings for the substitutional and interstitial Fe atom, as well as for different small clusters are well known [11–13];

(iv) the thermal equilibrium state of Au–Fe has been intensively studied using high-temperature Mössbauer spectroscopy combined with small angle x-ray scattering [12].

This study will be followed by small angle x-ray scattering and TEM at the same specimens [14].

2. Experimental procedure

Specimens with an Fe concentration of 1.0 at.% were prepared by electron-beam melting under ultra-high vacuum (10^{-9} mbar). The starting materials were 99.999% pure Au and 99% pure Fe (90% enriched in ^{57}Fe). Before alloying, pure Fe had been electron-beam melted for purification. The same starting materials had been used in the earlier Mössbauer study of Au–Fe alloys at high temperatures [12]. Foils with a thickness of 3 μm were obtained by cold rolling and were cut into pieces of 5 mm × 5 mm. For measurements of electrical resistivity four leads were attached to the foils.

In order to introduce He bubbles into the specimens α-particles were implanted at 55 °C by a 40 MeV cyclotron at Ispra in Italy. Thin Al foils of different thicknesses were placed in front of the specimen to vary the particle energy between 0 and 5.4 MeV in order to obtain a homogeneous distribution of implanted particles. The total concentration of He atoms was 1500 ppm. He bubbles were formed by annealing the specimens at 600 °C after the He implantation.

Proton irradiations were performed at 220 °C by a tandem accelerator at KFA Jülich. The irradiation temperature was chosen following earlier work [10] to obtain the maximum segregation efficiency. The proton energy was 2.3 MeV. The typical irradiation rate and the maximum proton dose were 2.2×10^{14} cm^{-2} s^{-1} and 1.3×10^{19} cm^{-2}, respectively. Experimental details about both the He implantation and proton irradiation have already been reported [10].

In order to monitor the segregation of Fe atoms in Au, the electrical resistivity was measured at 4.2 K following every experimental step.

After measuring the resistivity, Mössbauer measurements were performed. If not particularly mentioned, the measuring temperature was room temperature (290(3) K). Measurements at low temperatures between 5 and 300 K were performed by using a He-flow cryostat. A Mössbauer source of ^{57}Co-in-Rh with about 50 mCi was used for measurements with transmission geometry.

3. Results and assignment of Mössbauer lines

3.1. Mössbauer spectra after He implantation and proton irradiation

Figure 1 shows Mössbauer spectra of Au–1.0at.%Fe measured at room temperature, namely (a) after annealing at 600 °C, (b) after He implantation, (c) after irradiating an annealed sample without He bubbles up to 0.18 dpa (i.e., Frenkel defects per atom), (d) after proton irradiation of a sample with He bubbles to 0.23 dpa. The spectrum (a) consists of two components, a single Lorentzian and a small doublet. The isomer shifts and the quadrupole splittings for both components agree well with former results on annealed alloys [11, 12]. The fit parameters are summarized in table 1. The single line corresponds to isolated Fe atoms on substitutional sites and the doublet arises from Fe atoms adjacent to one other Fe atom at a nearest-neighbour site [11, 12]. Henceforth we call the first component a monomer and the latter a dimer.

Table 1. Mössbauer fit parameters.

Components	Isomer shift δ (mm s^{-1})	Quadrupole splitting ΔE_q (mm s^{-1})	Magn. splitting at 5 K H_{hf} (T)	FWHM Γ (mm s^{-1})
Monomer	0.64(1)	0.00(—)	21.5(5)	0.28(2)
Dimer	0.58(2)	0.73(1)	—	0.28(3)
Defect line (Fe complex)	0.12(2)	0.32(3)	35.0(5)	0.35 to 0.45(5)[a]

[a] The linewidths are different in different specimens.

The fraction† of iron atoms corresponding to the dimer component is 0.07(1) (table 2), i.e. smaller than that expected from a random distribution of Fe atoms, 0.11. This suggests the existence of short-range order of the Fe atoms in the Au matrix, in agreement with the results of high-temperature Mössbauer experiments [12].

After He implantation at 55 °C with a dose of 1500 ppm He, a new doublet at the left-hand side of the monomer line appeared in the spectrum (figure 1(b)) in addition to the monomer and dimer lines. The fractions for the monomer, dimer and new doublet are 0.65(2), 0.27(3) and 0.08(3), respectively (table 2). The new doublet has a more negative isomer shift relative to the other lines (related to a higher s-electron density) and a relatively large quadrupole splitting of 0.32 mm s^{-1} (table 1). The origin of this component will be deduced from the results of the proton irradiation; in the present section we call it the defect line. The fraction of the dimer doublet

† For the Mössbauer data the temperature dependence of the resonance intensities of all components follows the usual Debye behaviour in all our AuFe specimens. This implies that the Mössbauer fraction is identical to the number fraction of Fe atoms.

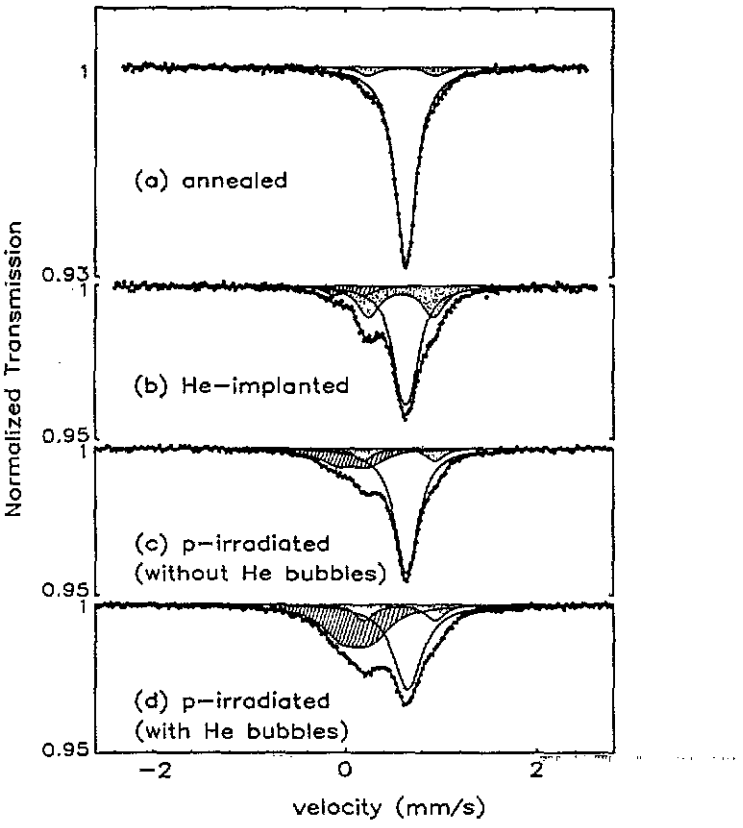

Figure 1. Room temperature Mössbauer spectra of Au–1.0 at.%Fe: (a) annealed at 600 °C; (b) after He implantation at 50 °C; (c) after proton irradiation at 220 °C without the bubbles up to 0.18 dpa (Frenkel defects per atom); (d) with He bubbles, formed by annealing at 600 °C after He implantation at 50 °C, and subsequent proton irradiation at 220 °C to 0.23 dpa. The single curve corresponds to monomers, the dotted doublet to dimers and the hatched doublet to the defect line.

Table 2. Fractions.

Specimen	p-dose (dpa)[a]	Fluence (dpa s^{-1})	Fractions			
			Monomer	Dimer	Fe complex	$-\Delta\rho/\rho$
Annealed at 600 °C	—	—	0.93(1)	0.07(1)	0.00(—)	0.00
He-implanted at 55 °C	—	—	0.65(2)	0.27(3)	0.08(3)	0.33
p-irradiated	0.18	3.0×10^{-6}	0.66(3)	0.10(2)	0.24(1)	0.49
p-irradiated (with He bubbles)	0.23	2.2×10^{-6}	0.47(2)	0.11(2)	0.42(1)	0.39

[a] 1 dpa (Frenkel defects per atom) corresponds to 7.3×10^{19} p cm^{-2}. The errors were obtained from a least-squares fitting using three components, namely monomer, dimer and Fe complex lines. A possible error due to neglecting small components in the spectrum is not included.

increased strongly after the implantation (cf figures 1(a) and (b)), whereas its isomer shift and quadrupole splitting did not change within the fitting errors.

In order to produce He bubbles, the He-implanted specimen was annealed at 600 °C for 1 h. After the annealing the Mössbauer spectrum showed the same profile as in figure 1(a), indicating that all Fe defects had re-dissolved and had returned into solution.

Finally, specimens without and with He bubbles were irradiated at 220 °C by protons with an energy of 2.3 MeV. The Mössbauer spectra for the specimens without and with He bubbles are presented in figures 1(c) and (d), respectively. Both spectra can be well analysed using three components: the monomer, dimer and defect lines with fractions of 0.66(3), 0.10(2) and 0.24(1) for the specimen without He bubbles (figure 1(c) and table 2) and 0.47(2), 0.11(2) and 0.42(1) for the specimen with He bubbles (figure 1(d) and table 2), respectively. The hyperfine parameters (isomer shift and quadrupole splitting) of the defect line for both spectra are the same as in the case of the He implantation before proton irradiation (figure 1(b)). The Mössbauer fitting parameters for the monomer, dimer and defect lines are summarized in table 1. In all spectra the linewidths of the defect line are broader than those of the monomer and dimer lines. This suggests a considerable perturbation from the environment which may differ in different specimens.

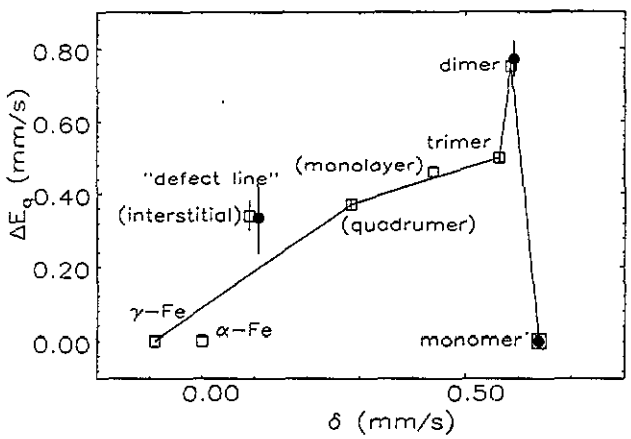

Figure 2. Correlation between quadrupole splittings and isomer shifts for different Fe complexes in Au: squares, earlier work [11–13, 15, 16]; circles, present results.

3.2. Interpretation of the defect line

In order to identify the nature of the defect line appearing in all spectra after irradiation, we show in figure 2 its Mössbauer parameters together with those for small substitutional Fe clusters such as monomer, dimer, trimer, quadrumer, γ-Fe (FCC), and α-Fe (BCC). The quadrupole splittings, ΔE_q, for different Fe clusters in Au are plotted as a function of the isomer shifts, δ. Each point in the plane of figure 2 corresponds to a certain Fe configuration in Au, yielding a different set of hyperfine parameters (isomer shift and quadrupole splitting). The data for the different points in figure 2 are taken from earlier results [11, 12, 15]. The lines between points are only drawn to show a tendency, i.e. to indicate how the point moves in the ΔE_q–δ plane when an Fe cluster grows in the Au matrix.

The simplest interpretation for the defect line would be that it originates from substitutional Fe clusters growing during irradiation. To test this hypothesis, we

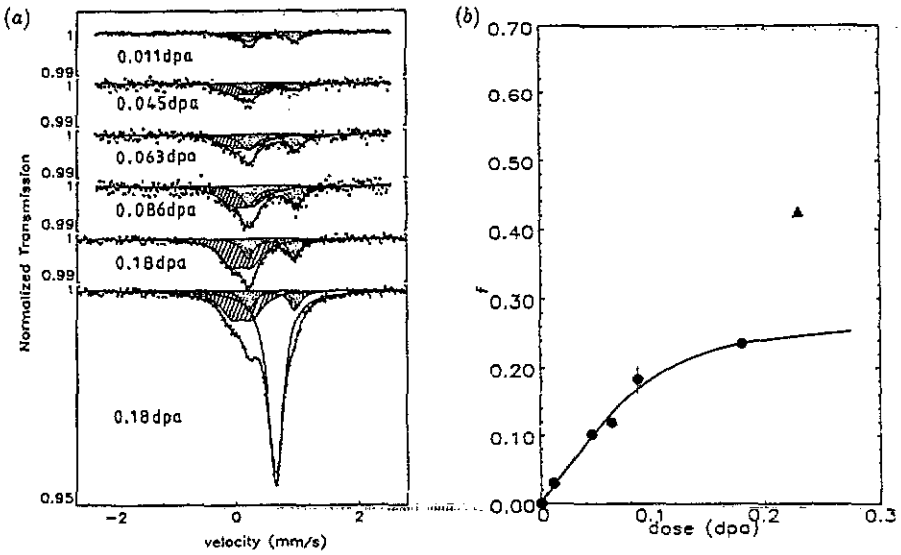

Figure 3. (*a*) Room temperature Mössbauer spectra of Au–1.0at.%Fe without He bubbles after proton irradiations with different proton doses. The full spectrum at the bottom is shown only for the specimen with the highest dose corresponding to 0.18 dpa. The other spectra were obtained by subtracting the monomer component from the full spectra. The areas under the Mössbauer lines are as in figure 1. (*b*) Fractions of defect line as a function of proton dose. The circles correspond to the specimen without He bubbles and the triangle to the specimen with He bubbles (0.23 dpa). The full curve is a guide to the eye.

Table 3. Proton dose dependence of fraction.

p-dose dpa	Fluence ($\times 10^{-6}$ dpa s^{-1})	Fractions			$-\Delta\rho/\rho$
		Monomer	Dimer	Fe complex	
0.011	1.6	0.90(1)	0.07(1)	0.03(2)	0.04
0.045	1.9	0.84(1)	0.06(1)	0.10(1)	0.26
0.063	1.8	0.78(1)	0.10(1)	0.12(1)	0.34
0.086	1.6	0.69(2)	0.13(1)	0.18(3)	0.43
0.18	3.0	0.66(3)	0.10(2)	0.24(1)	0.49

have irradiated the Au–1.0at.%Fe specimens without He bubbles with proton doses between 0.011 and 0.18 dpa (table 3). The Mössbauer spectra, which were obtained by subtracting the monomer component from the total spectra, are shown for the different proton doses in figure 3(*a*). The fractions for the defect line are presented in figure 3(*b*) as a function of the proton doses. It is clearly seen that the fraction of the defect line increases monotonically with increasing proton dose. However the isomer shifts and the quadrupole splittings do not change at all as can be seen in figure 3(*a*). If the defect line was due to *growing substitutional* Fe clusters (e.g. during a homogeneous nucleation process), the lines for the smaller clusters (trimer, quadrumer, etc) would appear first in the spectra, i.e. for small proton doses, and the further development of the Fe clusters could be followed in different spectra. However, no indication for such a development via intermediate states is observed in the spectra after increasing proton doses. Therefore we conclude that the defect line

does not originate from Fe clusters on substitutional sites.

We further plotted in figure 2 the values for an Fe monolayer in Au synthesized by Hosoito *et al* [16] through alternate deposition of Fe and Au, which has hyperfine parameters which are quite different from the defect line. We do not know the Mössbauer parameters for an Fe vacancy complex, which would possibly appear in the present investigation. The corresponding line has been sought by Nasu *et al* [17, 18] after quenching Au–^{57}Co(^{57}Fe), but has not yet been found even though clear recovery stages in both positron lifetime and electric resistivity have been observed during isochronal annealing experiments. Nasu and his co-workers concluded that the Mössbauer parameters for the Fe vacancy complex are not significantly different from those for monomer Fe in Au. We conclude therefore that the defect line neither originates from an Fe monolayer nor from an Fe vacancy complex.

The point in figure 2, which is closest to the hyperfine parameters of the defect line, finally corresponds to a line tentatively assigned to interstitial Fe, which has been found by in-beam Mössbauer spectroscopy [13], an implantation technique combining Coulomb excitation with recoil implantation. As the presence of iron at interstitial sites, surrounded by gold atoms only, is extremely unlikely at room temperature (where the Mössbauer measurements were performed), interstitial iron cannot be the origin of the defect line which has to correspond, therefore, to an unknown Fe complex. The structural pattern of this complex must be repeated as a 'motif' in regions of the sample where segregation takes place. We conclude this from the fact that the amount of defect lines increases with proton dose, whereas the hyperfine parameters do not change (figure 3). Alternatively, one could also interpret the defect line as the signature of a new (radiation-induced) Au–Fe phase corresponding to a periodic repetition of the 'motif'. Radiation-induced metastable phases have been observed, e.g. in proton-irradiated palladium-rich Pd–W alloys [19]. It is not possible, on the basis of our Mössbauer experiment, to decide between these two interpretations because they correspond to either a random or a periodic repetition of the 'motif'.

Moreover, the He bubbles do not appear to act as dominant sinks for Fe atoms because the same Mössbauer defect line is found in proton-irradiated samples with and without He bubbles (figure 1). The increase in the fraction of the defect line for the sample containing helium bubbles appears to arise only from the higher proton dose (figure 3(*b*)). The conclusion from this observation must be that the defects induced by proton irradiation, like cascades, act more effectively as sinks than the He bubbles.

3.3. Annealing experiments

Figure 4(*a*) shows the Mössbauer spectra of Au–1.0at.%Fe *without* He bubbles after proton irradiation, after annealing at 283 and 330 °C. In figure 4(*b*) analogous spectra of samples *with* He bubbles are shown. After annealing at 283 °C, the defect line nearly disappeared in specimens both without and with He bubbles, while the resonance intensity of the total spectrum remained constant. This implies that the Fe complexes were re-dissolved into substitutional Fe (monomers and dimers) in both specimens. Further annealing of both specimens at 330 °C finally led to spectra identical to those before proton irradiation, showing short-range order of Fe in the Au matrix. These observations are in accordance with the resistivity measurements that indicate the re-dissolution of the segregated Fe atoms in this temperature range (see table 4 and [10]).

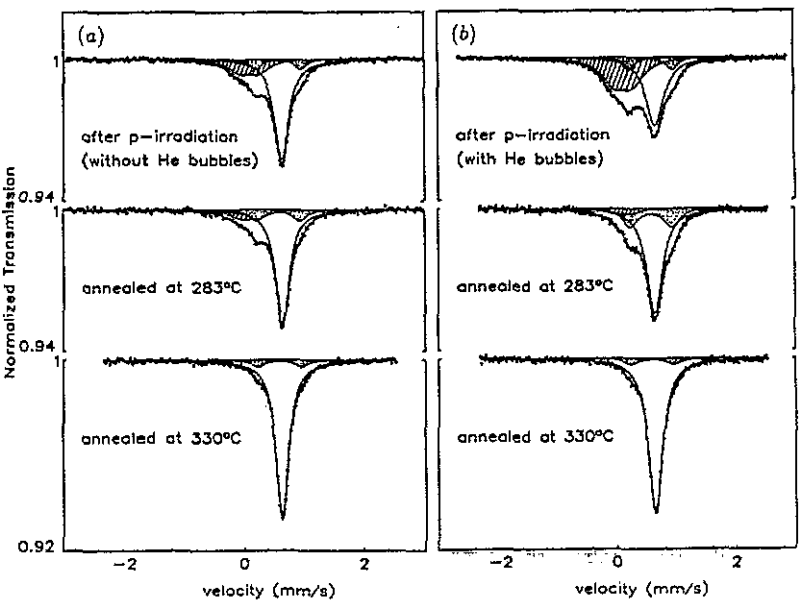

Figure 4. Room temperature Mössbauer spectra after annealings: Au–1.0at.%Fe (*a*) without He bubbles, and (*b*) with He bubbles. The areas under the Mössbauer lines are as in figure 1.

Table 4. Fractions after annealings.

Specimen	p-dose dpa	Fluence ($\times 10^{-6}$ dpa s^{-1})	Fractions			$-\Delta\rho/\rho$
			Monomer	Dimer	Fe complex	
Without He bubbles						
As irradiated	0.18	3.0	0.66(3)	0.10(2)	0.24(1)	0.49
Annealed at 275 °C	0.18	3.0	0.72(1)	0.14(1)	0.14(2)	0.40
Anealed at 330 °C	0.18	3.0	0.92(1)	0.08(1)	0.00(–)	0.06
With He bubbles						
As irradiated	0.23	2.2	0.47(2)	0.11(2)	0.42(1)	0.39
Annealed at 283 °C	0.23	2.2	0.69(2)	0.23(1)	0.08(2)	0.22
Annealed at 330 °C	0.23	2.2	0.93(1)	0.07(1)	0.00(—)	0.06

It appears noteworthy that the fraction of the dimers in both spectra (figure 4(*a*) and (*b*)) increased during the annealing at 283 °C (table 4). Such an additional formation of dimers is in striking contrast to the tendency for short-range order in Au–Fe at high temperatures [11, 12]. An explanation of this discrepancy would be that during re-dissolution of the segregated Fe, the iron concentration on substitutional sites and, therefore the dimer fraction, is temporarily increased in the vicinity of the segregations. Only when all the Fe atoms are again equally distributed throughout the matrix, the equilibrium state, i.e. short-range ordering, is attained (see table 4). The re-dissolution is due to a diffusion mechanism via thermal vacancies with a diffusion distance of Fe atoms in Au in the order of 10 Å h^{-1} at 283 °C [20], which makes this transient effect observable in the annealing experiment.

4. Magnetism

Low-temperature measurements were performed in order to gain more insight into the physical nature of the Fe segregations.

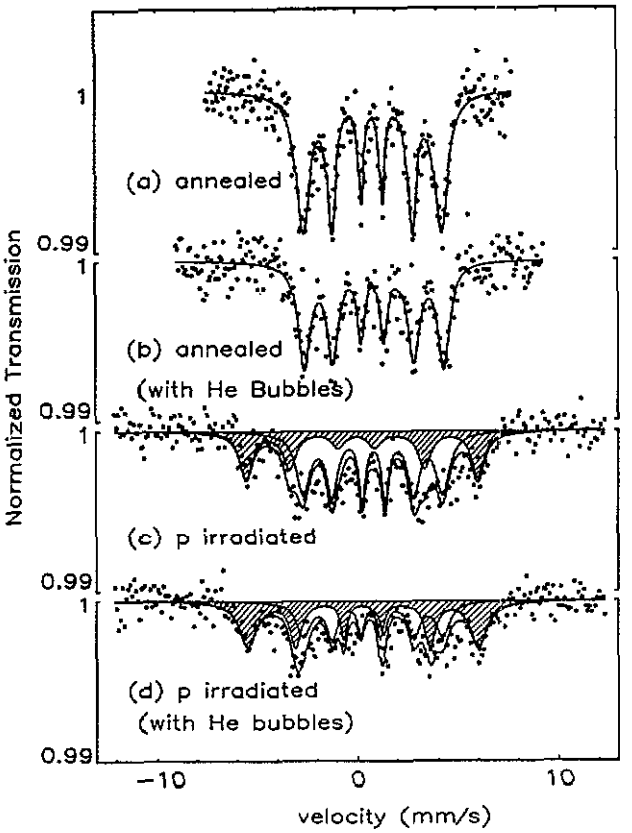

Figure 5. Mössbauer spectra measured at 5 K for Au–1.0at.%Fe: (*a*) annealed at 600 °C; (*b*) He-implanted and subsequently annealed at 600 °C (with He bubbles); (*c*) proton-irradiated up to 0.18 dpa (without He bubbles); and (*d*) proton-irradiated up to 0.23 dpa (with He bubbles). The hatched sextet corresponds to the component due to the Fe complexes.

The dilute alloy AuFe is well known as a spin-glass system, i.e. magnetic moments will be frozen below a freezing temperature, T_s, leading to an ordering of magnetic moments via s–d interaction [21]. The Mössbauer spectra in figures 5(*a*) and (*b*) were obtained from the samples of Au–1.0at.%Fe after annealing and after introducing He bubbles, respectively. At 5 K, both spectra have the same six-line magnetic splitting corresponding to a hyperfine field of 21.5 T in agreement with earlier results [22, 23].

After proton irradiation up to 0.18 and 0.23 dpa of the specimens without (figure 5(*c*)) and with He bubbles (figure 5(*d*)), respectively, the line-shapes of the Mössbauer spectra are clearly changed. Even though the statistics are rather poor, the computer fit unambiguously indicates the appearance of a new sextet (hatched in figure 5) at the expense of the already present sextet. The magnetic hyperfine field of the new component is the same for both spectra, namely 35.0(3) T. The isomer shift

and quadrupole interaction for the new sextet correspond to the defect line observed at room temperature (figures 1(c) and (d)); the fractions are 0.37(8) and 0.62(6) for the specimens without and with He bubbles, respectively, somewhat higher than the room-temperature data (0.24(1) and 0.42(1)). (The reason for this discrepancy might be that the substitutional dimer line could not be resolved as a separate sextet because of the poor statistics of the spectra and was therefore approximated by a broad line.)

In earlier Mössbauer experiments on Au–Fe alloys with high Fe concentrations, large hyperfine fields have been observed at 4.2 K [24]. The very large hyperfine field of 35.0 T found in the present investigation, which is even higher than for pure Fe (33.9 T [15]), roughly corresponds to the average hyperfine field in the spectra of Au–Fe with Fe concentrations of 30 to 40 at.% as found by Window [24]. However, Window's spectra, taken at room temperature, showed completely different shapes and the hyperfine parameters were different from those of the present room temperature spectra (figure 1). Accordingly, the very large hyperfine field cannot be due to Fe clusters containing a high concentration of Fe atoms on substitutional sites.

Measurements of the temperature dependence of the Mössbauer spectra were performed following the expectation that they would provide information on the magnetic interactions between Fe atoms in the different Fe configurations. As shown in figure 6(*a*), when increasing the temperature to 13 K the spectrum of non-irradiated Au–1.0at.%Fe containing He bubbles changed from a magnetic sextet to a single line, corresponding to a paramagnetic state. Violet and Borg [23] found a transition temperature of 11 K for Au–0.84 at.% Fe. The transition temperature is compatible with our result. The second component corresponding to the dimer could not be detected because of poor resolution due to a large velocity range.

Proton irradiation led to completely different spectra. They are shown in figure 6(*b*) for the temperature region between 5 and 30 K, and in figure 6(*c*) for temperatures between 40 and 290 K. (Notice that the velocity range of figure 6(*c*) is about a factor of 4 smaller than for figure 6(*b*).) Although the statistics are poor, especially for the spectra below 30 K (figure 6(*b*)), it can be seen in the spectra that the magnetic components remain up to 25–30 K (figure 6(*b*)). Above 30 K the spectra can be fitted assuming a monomer, a dimer and a defect line as in the case of room temperature, the width of these lines decreasing with temperature.

The most striking difference between spectra before and after proton irradiation is: before irradiation a sharp magnetic transition temperature $T_c(\simeq 13\ \mathrm{K})$ exists, whereas after irradiation the transition occurs over a broad temperature region. The sharp transition is known to be due to the magnetic interaction between substitutional Fe atoms via s–d interaction (spin glass) [21]. The broad transition might be related to the presence of several types of magnetic interactions:

(i) the strong exchange interaction between Fe atoms inside Fe segregations;

(ii) the weak magnetic interaction between the total magnetic moments of the Fe segregations; and

(iii) the interaction of those moments with the Fe atoms remaining dissolved in the Au matrix.

5. Discussion

After proton irradiation of Au–1.0at.%Fe alloy at 220 °C, a new Mössbauer line

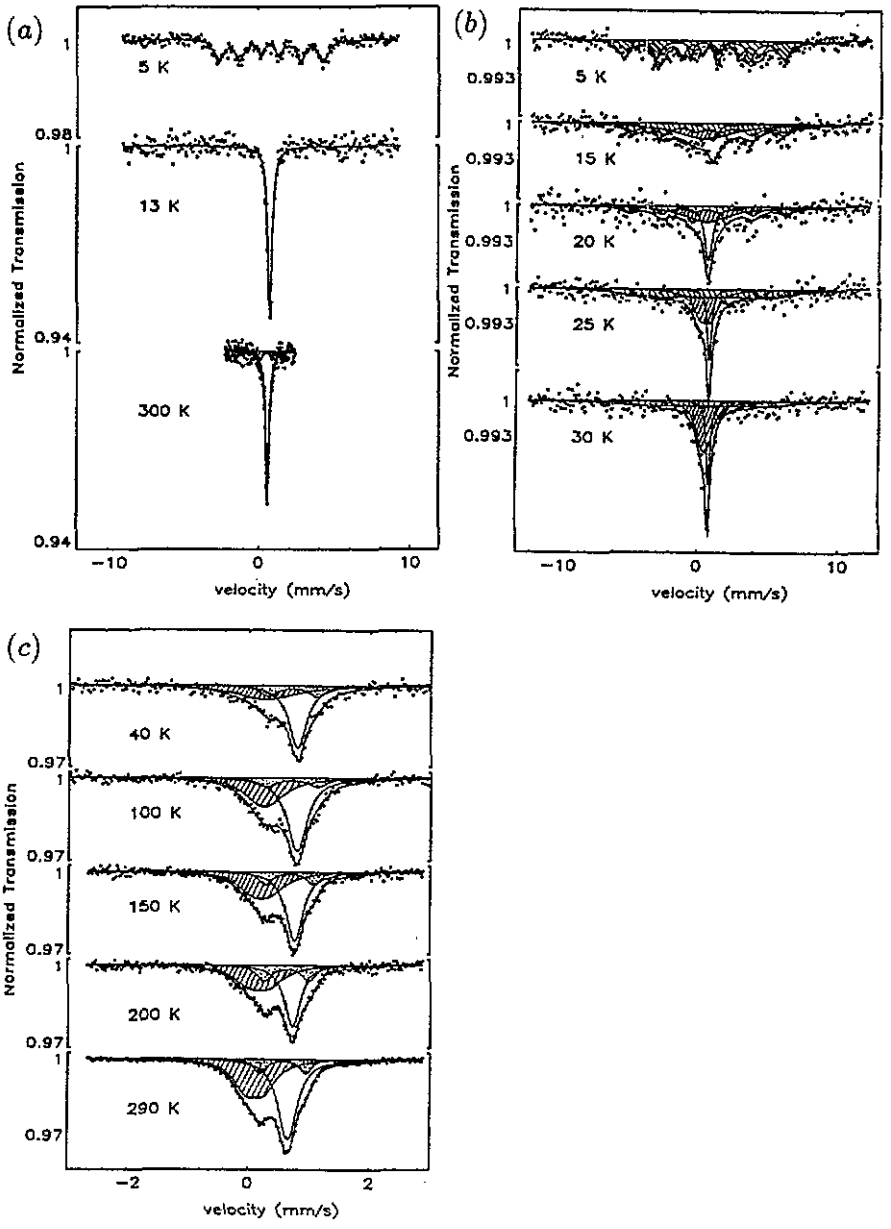

Figure 6. Low-temperature Mössbauer spectra of Au–1.0at.%Fe: (*a*) He implanted and subsequently annealed at 600 °C leading to the formation of He bubbles; (*b*) and (*c*) proton-irradiated up to 0.23 dpa. Note that the velocity range of (*c*) is a factor of four smaller than that of (*a*) and (*b*). The areas under the Mössbauer lines are as in figure 1.

appeared: its resonance intensity increases with increasing dose, and the hyperfine parameters of this line, which are similar to those of an Fe interstitial in Au, do not depend on the irradiation dose. Therefore, in section 3.2 we assigned the new line to an Fe complex repeated as a 'motif' in the Fe segregation. This can be compared with results from complementary experiments, i.e. electrical resistivity [10] and small-angle

x-ray scattering [14], both of which have been performed on the same specimens used for the present Mössbauer study.

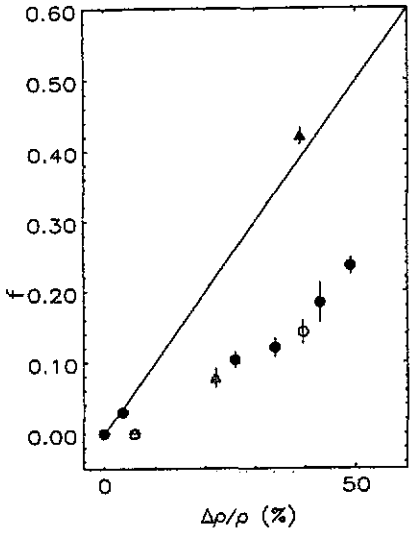

Figure 7. Mössbauer fractions of Fe complexes as a function of the irradiation-induced relative resistivity decrease. Full triangle and open triangles correspond to specimens with He bubbles after proton irradiation and after annealings, respectively. Full circles are obtained from specimens without He bubbles after proton irradiations with different doses and open circles from the specimen irradiated to 0.18 dpa and subsequently annealed.

Electrical resistivity has been measured at every experimental step to monitor the Fe fraction in solution in the Au matrix. The measurements were performed at 4.2 K [10]. The results are summarized in figure 7 in comparison with the results from the Mössbauer measurements. The fractions of the Fe complexes deduced from the Mössbauer spectra are plotted as function of the relative resistivity changes. The fractions determined by the resistivity measurement are considerably larger than those determined by Mössbauer spectroscopy (figure 7).

For the resistivity data the following assumptions have been made [10] in order to deduce the Fe fraction in solid solution:

(i) the segregated iron does not contribute to the resistivity;
(ii) each iron atom on a substitutional site contributes linearly to the resistivity.

If segregations were composed only of the Fe complexes (seen in the Mössbauer spectra), the Mössbauer fraction and the relative resistivity change should be equal. Evidently this is not the case (figure 7). We conclude, therefore, that the Fe segregations must also contain Fe atoms on substitutional sites (monomers and dimers) which do not contribute to the resistivity.

Since Mössbauer spectroscopy is a short-sighted method (i.e. the hyperfine parameters are mainly determined by the nearest-neighbour atoms), the influence from the neighbouring Fe atoms (like monomers, dimers, Fe complexes) on the hyperfine parameters of the Fe complex in the Fe segregations does not lead to new Mössbauer

lines, but to some line broadening instead†. The line-broadening mentioned in section 3.1 may be caused by such different configurations in the Fe segregations.

Furthermore, the small-angle x-ray scattering [14] would offer information on the size of each Fe segregation, which is complementary to the present Mössbauer study concerning the constituents of the Fe segregation. The result after proton irradiation, indeed, shows a considerable enhancement of the intensity of small-angle scattering suggesting the formation of the Fe segregation in Au matrix. A detailed analysis will be presented in a separate publication [14].

6. Conclusion

Proton irradiation of Au–1.0at.%Fe at 220 °C induces segregation of Fe atoms, even though substitutional Fe in Au has a tendency towards short-range ordering [12]. Mössbauer spectroscopy and electrical resistivity provide atomistic information, both on the Fe segregation process (namely the constituents of the segregation) and on the Fe atoms in the Au matrix. As shown by electrical resistivity measurements, about 50% of all Fe atoms segregate after proton irradiation up to 0.18 dpa. Comparing these results with the Mössbauer spectroscopy data we must conclude that the segregations contain the same amount (i.e. 25% of the total number of Fe atoms in the sample) of small Fe complexes and substitutional Fe atoms. The hyperfine parameters of the Fe complex, which are close to those of interstitial Fe in Au [13], do not show any proton dose dependence. The Fe complex is, therefore, repeated as a 'motif' in the Fe segregations, a fact that could also be interpreted as the appearence of a new, metastable Au–Fe phase. Moreover, the magnetic properties of Au–Fe are strongly influenced by the radiation-induced segregation. Indeed, the magnetic splitting of the Mössbauer lines at low temperatures disappears more gradually and at higher temperatures after proton irradiation. Finally, it is interesting to note that the introduction of He bubbles as additional defect sinks did not change the Mössbauer parameters corresponding to the Fe 'motif', but only its amount.

Acknowledgments

W Schilling, P Ehrhart, H G Haubold and K Schroeder are greatly acknowledged for valuable discussions. One of the authors (YY) thanks S Nasu, Osaka University Japan, for fruitful discussions. The authors would like to thank Mr Franke, Hahn–Meitner Institut Berlin, for the specimen preparation, D Tuppinger and F Langmayr for experimental help and the technical staff of the cyclotron at Ispra and Tandetron IFF for performing the irradiations. Part of this work was supported by Fonds zur Förderung der Wissenschaftlichen Forschung (P6733P), Austria.

References

[1] Russel K C 1984 *Prog. Mater. Sci.* 28 229

† In Au–Fe alloys [12] with Fe concentrations between 1 and 15 at.%, a perturbation from Fe atoms on second and third neighbours could be detected in Mössbauer spectra only as line broadening.

[2] Anthony T R 1972 *Radiation-Induced Voids in Metals and Alloys (US Atomic Energy Commission Publication No CONF 710601)* ed J W Corbett and L C Ianiello p 630
[3] Okamoto P R and Rehn L E 1979 *J. Nucl. Mater.* **83** 2
[4] Averback R S, Rehn L E, Wagner W, Wiedersich H and Okamoto P R 1983 *Phys. Rev.* B **28** 3100
[5] Hashimoto T, Rehn L E and Okamoto P R 1988 *Phys. Rev.* B **38** 12868
[6] Wollenberger H 1987 *Mater. Sci. Forum* **15–18** 1363
[7] Ezawa T, Kiritani M and Fujita F E 1988 *J. Nucl. Mater.* **155–7** 179
[8] Erck R A and Rehn L E 1989 *J. Nucl. Mater.* **168** 208
[9] Murphy S M 1989 *Phil. Mag.* A **59** 953
[10] Vaessen P, Ehrhart P, Höfer H, Jäger W, Keldenich D, Schilling W and Weckermann B 1987 *Mater. Sci. Forum* **15–18** 623
Vaessen P 1988 *Dissertation* T H Aachen
[11] Whittle G L and Campbell S J 1985 *J. Phys. F: Met. Phys.* **15** 693
[12] Yoshida Y, Langmayr F, Fratzl P and Vogl G 1989 *Phys. Rev.* B **39** 635;
Fratzl P, Langmayr F and Yoshida Y 1991 *Phys. Rev.* B **44** 4192
[13] Menningen M, Sielemann R, Yoshida Y and Vogl G 1992 in preparation
Yoshida Y 1989 *Hyperfine Interact.* **47** 95
[14] Höfer H 1991 *Dissertation* T H Aachen
[15] Preston R S, Hanna S S and Heberle J 1962 *Phys. Rev.* **128** 2207
[16] Hosoito N, Ogawa S and Shinjo T 1990 *Hyperfine Interact.* **57** 1865
[17] Tanaka I, Nasu S and Fujita F E 1988 *J. Phys. Soc. Japan* **57** 585
[18] Nasu S 1988 *Hyperfine Interact.* **40** 135
[19] Weaver L and Ardell A J 1980 *Scr. Met.* **14** 765
[20] Duhl D N, Hirano K and Cohen M 1963 *Acta Met.* **7** 86
[21] Mydosh J A 1978 *J. Magn. Magn. Mater.* **2** 237
Meyer C and Hartmann-Boutron F 1990 *Hyperfine Interact.* **59** 219
[22] Ridout M S 1969 *J. Phys. C: Solid State Phys.* **2** 1258
[23] Violet C E and Borg R J 1966 *Phys. Rev.* **149** 540
Violet C E and Borg R J 1983 *Phys. Rev. Lett.* **51** 1073
[24] Window B 1972 *Phys. Rev.* B **6** 2013